

Formation cross sections of isotopes of the superheavy nuclei Og, Fl, and Nh using the dinuclear system model

M. R. Pahlavani  and M. Masoumi Dinan*

Department of Nuclear Physics, Faculty of Basic Science, University of Mazandaran, P.O. Box 47415-416, Babolsar, Iran

 (Received 23 July 2020; revised 26 December 2020; accepted 15 February 2021; published 11 March 2021)

Using the double-folding potential based on the dinuclear system model, the production cross section of different even isotopes of Og through $^{84-92}\text{Kr} + ^{208}\text{Pb} \rightarrow ^{292-300}\text{Og}$, various even isotopes of Fl through $^{72,74,76}\text{Ge} + ^{208}\text{Pb} \rightarrow ^{280,282,284}\text{Fl}$, ^{279}Nh and ^{278}Cn through interaction of ^{70}Zn with ^{208}Pb and ^{209}Bi cold reactions are calculated. To evaluate the nuclear temperature of these compound nucleus, the exact Ginzburg-Landau theory is employed. Calculated formation cross section for different isotopes of Og, Fl, Nh, and Cn using complete set of potentials consisting of nuclear double-folding, Coulomb, and centripetal potentials are compared with the results of other theoretical models as well as available experimental data. The comparison indicates that the calculated formation cross section using this approach agreed well with experimental data and the results of other theoretical models.

DOI: [10.1103/PhysRevC.103.034608](https://doi.org/10.1103/PhysRevC.103.034608)

I. INTRODUCTION

The first attempt for synthesis of super heavy nuclei (SHN) has been provided by Fermi [1]. He observed elements with atomic numbers above $Z = 92$. Over the years, improvement in the experimental instruments made it possible to produce heavier elements using energetically charged particles provided with sophisticated accelerators. Transuranium and SHN with the interaction of these energetic beams like ^{48}Ca on heavy nuclei have been produced. Several experimental procedures have been used to generate each SHN, for example, successive neutrons absorption of heavy elements, the interaction of accelerated heavy charged particles, and a combination of them. The synthesis of the SHN is a very important subject since heavy and superheavy nuclei provided significant improvements of nuclear physics which can be referred to the production of nuclear energy [2–5]. In spite of numerous theoretical and experimental investigations that have been done for the production of SHN in the last century, this subject is still an important open research title of both experimental and theoretical nuclear physics. Recently, production of SHN has attracted the attention of nuclear physicists. Despite the large number of superheavy families that are detected, there are still many SHN under study, and research on their properties is a time consuming process. Advances in nuclear structure models have led to the emergence of the concept of an island of stability existing near the next spherical doubly magic nucleus heavier than the ^{208}Pb nucleus. The synthesis of superheavy elements ($Z \leq 113$, $N \leq 165$) was carried out by stable neutron-rich projectiles heavier than ^{64}Ni or ^{70}Zn with lead and bismuth targets in cold fusion reactions and ^{232}Th , ^{238}U , and $^{242,244}\text{Pu}$ targets were also applied to

synthesize the SHN with atomic numbers $Z = 110, 112$, and 114 in hot fusion reactions [6–8], respectively. Four new isotopes of $Z = 112$ element and 14 new isotopes of new elements with $Z = 113–116$ in which neutron numbers are closer to the predicted spherical shell closure at $N = 184$ were identified using a new method at the Flerov Laboratory of Nuclear Reactions (FLNR) of the Joint Institute for Nuclear Research (JINR), Russia about a decade ago [9–12]. The experiments using fusion reactions of the ^{48}Ca projectile with radioactive ^{249}Bk target nuclei were applied to produce the $^{293}117$ and $^{294}117$ SHN isotopes, respectively. In order to produce ^{249}Bk , intense neutron irradiation of Cm and Am targets during approximately 250 days in the high flux isotope reactor was performed at Oak Ridge National Laboratory (ORNL), Japan. According to the studies on the Bk SHN by the radiochemical engineering development center of ORNL, product contains 22.2 mg of ^{249}Bk , only 1.7 ng of ^{252}Cf , and no other detectable impurities. The Og ($Z = 118$) SHN was discovered in 2006 [13]. Attempts have also been made to obtain the formation cross section of elements 119 and 120 in the fusion-evaporation reactions of ^{209}Bi and ^{208}Pb targets with ^{86}Cr and ^{88}Sr projectiles, respectively [14]. Today, the production cross section of SHN has been studied with many theoretical models such as the dynamical Langevin model, the DNS model, the fluctuation dissipation model, the nuclear collectivization concept, the macroscopic dynamical model, and the multidimensional stochastic model [15–17]. The production cross section and the lifetime of corresponding SHN rapidly decrease with the enhancement of the charge number Z of the target nucleus. To understand the fusion of heavy energetic nuclei for the production of SHN, many theoretical models have been developed, and some experiments have been performed [18–23]. Among various theoretical models, the DNS model has made significant progress in reproducing the available experimental data [24]. According to the

*m.pahlavani@umz.ac.ir

DNS model, the formation of the SHN is described as a competitive process between quasifission and complete fusion via nucleon transfer. It is assumed that the DNS evolves along with two coordinates: (i) R coordinates (center to center distance between the reacting nuclei). (ii) The collective coordinate of mass asymmetry $\eta = (A_1 - A_2)/(A_1 + A_2)$ with A_1 and A_2 as the mass numbers of the DNS nuclei. Evolution of the R coordinate leads to the quasifission process, while variation of η results in the well-known compound nucleus formation [25,26]. Substantial information about the SHN, including formation cross section, fusion and fission barriers, and the survival probability, is obtained by studying the fission processes. The resultant compound nucleus is formed in an excited state, and it may undergo fission or emits one or more particles and γ radiations. This model not only reproduces the experimental data quite well but also predicts the optimal projectile-target combination as well as the optimal bombarding energy to form certain SHN. It has been shown that the effects of isotopic dependence and deformation of projectile and target on the formation cross section of SHN are essential. The nuclear level density is a fundamental quantity for research in different areas of nuclear physics. One of the basic quantities for calculating the formation cross section of SHN is nuclear level density. Several models have been developed to calculate this temperature dependent quantity, namely the simple Fermi gas (FG) model [26], the back-shifted Fermi gas (BSFG) model [27–29] with constant temperature (CT), and temperature-dependent level density [30] directly yield the nuclear level density and shell model Monte Carlo (SMMC) method [31,32], Bardeen-Cooper-Schrieffer (BCS) approach [33], and static path plus random phase approximation (SPA + RPA) [34,35] produce it indirectly through fundamental laws of classical thermodynamics. This temperature dependent quantity can be evaluated directly or indirectly through fundamental laws of classical thermodynamics. In the BSFG model, the back shifted parameter is a free parameter that is obtained by fitting to experimental data. The pairing energy is expressed as a constant term in the BSFG model, however the temperature-dependent liquid drop model [36] considers it as a function of the nuclear temperature. The BCS theory [37] predicts the decrease in pairing energy with the growth of temperature [38,39]. This point can be included in the usual BSFG model through the new version of Ginzburg-Landau (GL) theory of phase transitions, namely the exact Ginzburg-Landau (EGL) theory [40,41] which is appropriate for describing the thermal properties of nuclei. In this model, the importance of paired phase at different temperatures is indicated by the order parameter. The rest of the paper is organized as follows. In Sec. II, the formulation cross section of SHN in the base of the DNS model using the double-folding potential is presented. Moreover, the EGL formula is introduced to calculate the pairing energy. The formation cross sections of $^{292-300}\text{Og}$, $^{280,282,284}\text{Fl}$, ^{278}Cn , and ^{279}Nh isotopes are computed using the double-folding nuclear potential. The calculated results of formation cross sections are compared with other theoretical as well as available experimental data. Finally, significant conclusions are presented in Sec. IV.

II. DESCRIPTION OF THE THEORETICAL MODELS

The DNS model is a two-step process which starts with complete fusion of colliding nuclei to overcome the Coulomb barrier between the projectile and target and the formation of a heavy compound nucleus, followed by de-excitations of the obtained compound nucleus, leads to the formation of evaporation residues, the nuclei in the vicinity of the ground state, and also fission. The transmission probability in the fusion stage of the projectile and target is dependent on the incident energy and relative angular momentum. Well-known quantum mechanical penetration probability has played an important role in this stage, especially at incident energies below the fusion barrier. Fusion barrier distribution is used to reproduce fusion cross sections. Therefore, according to the DNS model, the evaporation residue cross section, $\sigma_{ER}(E_{c.m.})$ is usually expressed as a sum over all partial waves J at the center of mass energy $E_{c.m.}$ [42],

$$\sigma_{ER}(E_{c.m.}) = \sum \sigma_C(E_{c.m.}, J) P_{CN}(E_{c.m.}, J) W_{\text{sur}}(E_{c.m.}, J). \quad (1)$$

In this equation, σ_C is the partial wave capture cross section responsible for the transition of the projectile nucleus through the entrance Coulomb barrier and the formation of DNS. P_{CN} is the formation probability of the compound nucleus as a configuration of two touching DNS after the capture stage into a spherical or nearly spherical form of the compound nucleus. W_{sur} is the survival probability of formed compound nucleus against fission. Equation (1) can be rewritten approximately as [43]

$$\sigma_{ER}(E_{c.m.}) = \sigma_C(E_{c.m.}) P_{CN}(E_{c.m.}) W_{\text{sur}}(E_{c.m.}). \quad (2)$$

The capture cross section is determined using [43,44]

$$\sigma_C(E_{c.m.}) = \frac{\pi \hbar^2}{2\mu E_{c.m.}} (J_{\text{max}} + 1)^2 T(E_{c.m.}), \quad (3)$$

where μ is the reduced mass of target and projectile, and J_{max} is the effective maximal angular momentum of the compound nucleus. $J_{\text{max}} = 10$ in units of \hbar and $T(E_{c.m.}) = 0.5$ seem to be reasonable for our calculation [43]. The following formula is used to calculate the probability of the formation of a compound nucleus [43]:

$$P_{CN} = \frac{\lambda_\eta}{\lambda_\eta + \lambda_R} - \frac{\lambda_\eta \lambda_R}{\lambda_\eta + \lambda_R} \frac{\tau_\eta - \tau_R}{\beta} \quad (4)$$

with $\beta = e - 1 \approx 1.72$. The first term in Eq. (4) comes from the contribution of the quasistationary width. Also, the second term depends on the transition times, τ_i , and can be evaluated using [21]

$$\tau_R = \frac{\hbar}{\Gamma} \ln(10B_{qf}/T), \quad (5)$$

$$\tau_\eta = \frac{\Gamma}{2\hbar\omega_\eta^2} \ln(10B_{fus}^*/T). \quad (6)$$

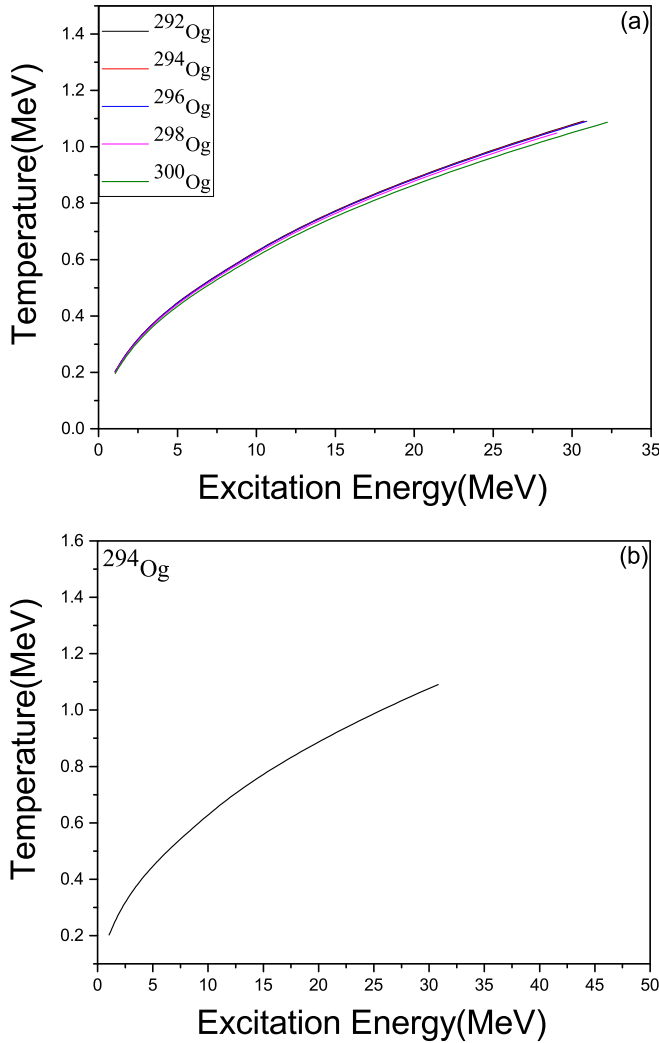


FIG. 1. Nuclear temperature as a function of excitation energy for (a) ^{292}Og , ^{294}Og , ^{296}Og , ^{298}Og , ^{300}Og isotopes and (b) ^{294}Og .

λ_i is the multidimensional Kramers rate and is evaluated by using [43,45]

$$\lambda_i = \frac{1}{2\pi} \frac{\omega_i^2}{\omega_i^{B_R} \omega_i^{B_\eta}} \left(\sqrt{\left(\frac{\Gamma}{\hbar}\right)^4 + 4(\omega_i^{B_R} \omega_i^{B_\eta})^2} - \left(\frac{\Gamma}{\hbar}\right)^2 \right)^{\frac{1}{2}} e^{-\frac{B_i}{T}}, \quad (7)$$

where B_i is the height of fusion ($B_\eta = B_{fus}^*$) or quasifission ($B_R = B_{qf}$) barrier. Here, $\omega_i^{B_j}$ ($i, j = R, \eta$), ω_i and Γ are the frequencies of inverted harmonic oscillators approximating the potentials in variables, R and η , near the top of the barrier, the oscillator frequencies approximating the potentials in the initial configuration of DNS, and the average doubled width of single particle states, respectively. The quantity $\omega_i^{B_R}$ is calculated using [45]

$$\omega_i^{B_j} = \sqrt{\left| \frac{\partial^2 U(R, \eta, J)}{\partial i^2} \right|_{B_j}} / \mu_{ii}, \quad (8)$$

TABLE I. The deformation parameters β_2 , β_3 , β_4 , and β_6 are the quadrupole, octupole, hexadecapole, and hexacontatetrapole deformation parameters [56], respectively.

nucleus	β_2	β_3	β_4	β_6
^{208}Pb	0.000	-0.013	0.000	0.000
^{209}Bi	-0.008	-	0.008	-0.002
^{70}Zn	0.045	-	0.001	0.001
^{72}Ge	-0.224	-	-0.034	0.005
^{74}Ge	-0.224	-	-0.041	0.001
^{76}Ge	0.143	-	0.008	-0.004
^{84}Kr	0.062	-	-0.007	0.001
^{86}Kr	0.053	-	-0.007	0.000
^{88}Kr	0.062	-	0.001	0.000
^{90}Kr	0.162	-	0.001	-0.007
^{92}Kr	0.228	-	-0.019	-0.024

where μ_{RR} and $\mu_{\eta\eta}$ are the mass parameters and are evaluated using [20]

$$\mu_{RR} = \frac{Am(1-\eta^2)}{4} \left(1 - \frac{\nu}{1-\eta^2} \right)^{-1}, \quad (9)$$

$$\mu_{\eta\eta} = \frac{2\sqrt{2\pi}b^2Am}{\nu}, \quad (10)$$

where $b = 1$ fm and ν is defined as

$$\nu = \frac{1}{A} (\xi_0 - \xi_1 \eta^2) (1 - \xi s), \quad (11)$$

where $s = R - R_1 - R_2$ in which R , R_1 , and R_2 show the radii of nuclei and we used the values $\xi_0 = 16$, $\xi_1 = 17.5$, $\xi = 0.3 \text{ fm}^{-1}$.

The potential energy of DNS is evaluated using

$$U(R, \eta, Z_1, Z_2, J) = B_1 + B_2 + V(R, J) - [B_{12} + V_{\text{rot}}(J)], \quad (12)$$

where B_1 , B_2 , and B_{12} are the binding energies of fragments and the compound nucleus, respectively. $V(R, J)$ is the nucleus-nucleus interacting potential and is calculated using

$$V(R, Z_1, Z_2, A_1, A_2, J) = V_N + V_C + \frac{\hbar^2 l(l+1)}{2\mu r^2}. \quad (13)$$

Here, the Coulomb potential, V_C is defined as follows [46]:

$$\begin{aligned} V_C(r, Z_1, Z_2, A_1, A_2) &= \frac{Z_1 Z_2 e^2}{R} \\ &+ \left(\frac{9}{20\pi} \right)^{\frac{1}{2}} \left(\frac{Z_1 Z_2 e^2}{R^3} \right) \sum_{i=1}^2 R_i^2 \beta_i P_2(\cos \theta_i) \\ &+ \left(\frac{3}{7\pi} \right) \left(\frac{Z_1 Z_2 e^2}{R^3} \right) \sum_{i=1}^2 R_i^2 [\beta_i P_2(\cos \theta_i)]^2, \end{aligned} \quad (14)$$

where θ_i is the angle between radius vector \vec{R} and the symmetry axis of the i th nucleus. R_i and β_i are the radius and the quadrupole deformation of the i th nucleus. For nuclear interaction, the double-folding potential [47–50] is used. The

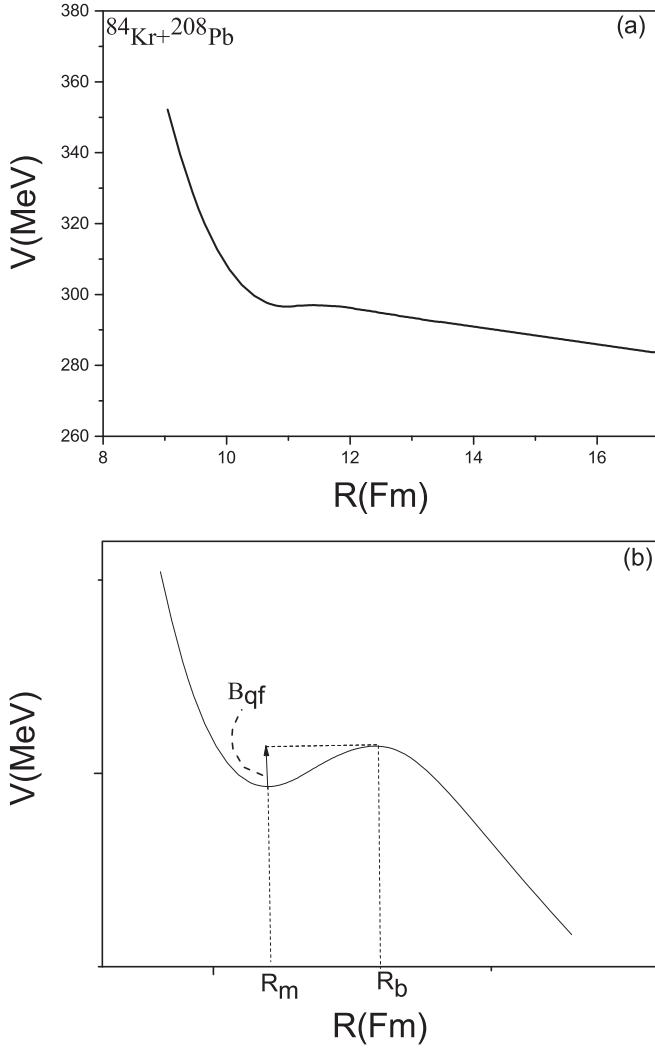


FIG. 2. Nucleus-nucleus potential as a function of distance for (a) the $^{84}\text{Kr} + ^{208}\text{Pb}$ reaction and (b) the schematic representation of the nucleus-nucleus potential as a function of distance.

nuclear double-folding potential, V_N is defined as follows [51,52]:

$$V_N(A_1, A_2) = C_0 \left\{ \frac{F_{in} - F_{ex}}{\rho_{00}} \left[\int \rho_1^2(\vec{r}) \rho_2(\vec{r} - \vec{R}) d\vec{r} + \int \rho_1(\vec{r}) \rho_2^2(\vec{r} - \vec{R}) d\vec{r} \right] + F_{ex} \int \rho_1(\vec{r}) \rho_2(\vec{r} - \vec{R}) d\vec{r} \right\}, \quad (15)$$

where $F_{in,ex}$ is obtained using

$$F_{in,ex} = f_{in,ex} + f'_{in,ex} \frac{N_1 - Z_1}{A_1} \frac{N_2 - Z_2}{A_2}, \quad (16)$$

where $N_{1,2}$ and $Z_{1,2}$ are neutron and proton numbers of the two interacting nuclei, respectively. Here, $C_0 = 300 \text{ MeV fm}^3$, $f_{in} = 0.09$, $f_{ex} = -2.59$, $f'_{in} = 0.42$, $f'_{ex} = 0.54$,

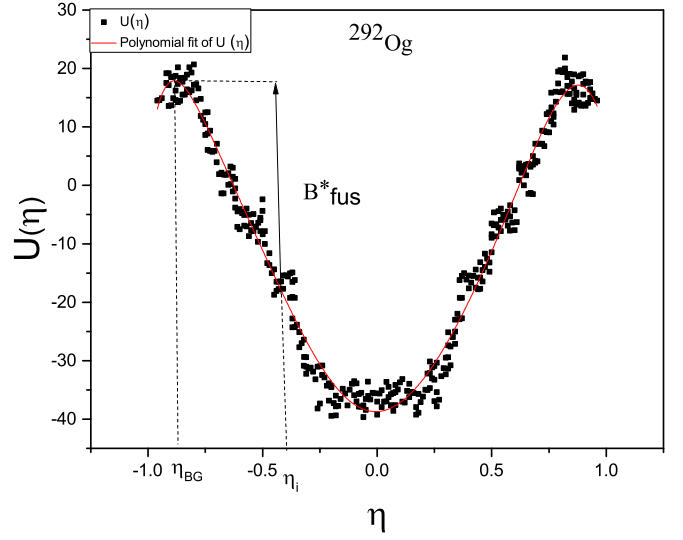


FIG. 3. Potential energy of DNS as a function of η .

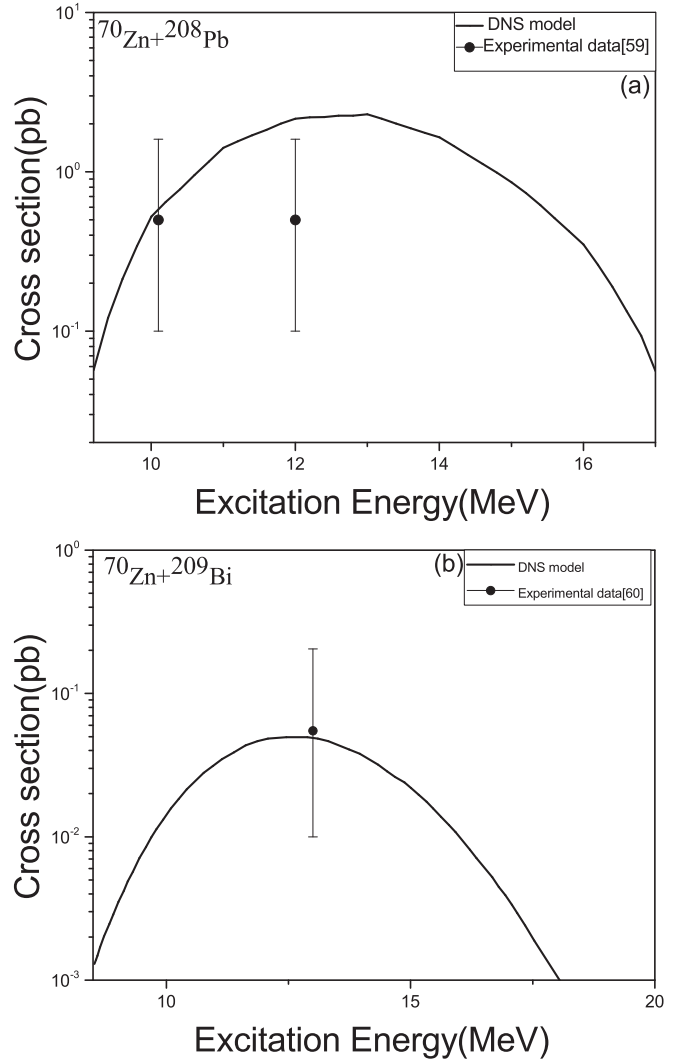


FIG. 4. Calculated evaporation residue cross section are compared with experimental data [59,60] for (a) $^{70}\text{Zn} + ^{208}\text{Pb}$ and (b) $^{70}\text{Zn} + ^{209}\text{Bi}$ reactions.

TABLE II. The evaporation residue cross section, σ_{ER}^1 , σ_{ER}^2 , and σ_{ER}^3 are our calculated cross section, results presented in Refs. [25] and [57], respectively.

Reactions	E^* (MeV)	σ_{ER}^1	σ_{ER}^2	σ_{ER}^3
$^{70}\text{Zn} + ^{208}\text{Pb} \rightarrow ^{277}\text{Cn} + 1n$	9.8	0.34 pb	1.8 pb	–
$^{72}\text{Ge} + ^{208}\text{Pb} \rightarrow ^{279}\text{Fl} + 1n$	12.6	200 fb	–	–
$^{74}\text{Ge} + ^{208}\text{Pb} \rightarrow ^{281}\text{Fl} + 1n$	12.5	110 fb	100 fb	–
$^{76}\text{Ge} + ^{208}\text{Pb} \rightarrow ^{283}\text{Fl} + 1n$	12.4	210 fb	200 fb	–
$^{84}\text{Kr} + ^{208}\text{Pb} \rightarrow ^{291}\text{Og} + 1n$	12.5	1.94 fb	1.7 fb	–
$^{86}\text{Kr} + ^{208}\text{Pb} \rightarrow ^{293}\text{Og} + 1n$	13.3	4.78 fb	5.1 fb	4.6 fb
$^{88}\text{Kr} + ^{208}\text{Pb} \rightarrow ^{295}\text{Og} + 1n$	12	3.43 fb	4.1 fb	–
$^{90}\text{Kr} + ^{208}\text{Pb} \rightarrow ^{297}\text{Og} + 1n$	13.1	0.55 fb	1.2 fb	–
$^{92}\text{Kr} + ^{208}\text{Pb} \rightarrow ^{299}\text{Og} + 1n$	12.4	0.26 fb	1 fb	–

and $\rho_{00} = 0.17 \text{ fm}^{-3}$ are considered. ρ_1 and ρ_2 represent two-parameter Fermi nuclear density [53]. In order to find the isotopic composition of the DNS, the equilibrium condition of N/Z in the system is applied as follows [45]:

$$N/Z = \frac{N_1/Z_1 + N_2/Z_2}{2}, \quad (17)$$

where N_1 , N_2 and N are the neutron number of fragments and the compound nucleus and Z_1 , Z_2 and Z are the charge number of fragments and the compound nucleus, respectively. The survival probability is calculated using

$$W_{\text{sur}}(E^*) = P_{1n}(E^*) \frac{\Gamma_n(E^*)}{\Gamma_n(E^*) + \Gamma_f(E^*)}, \quad (18)$$

where Γ_n and Γ_f are the partial widths of neutron emission and fission, respectively, and P_{1n} is evaluated as follows:

$$P_{1n}(E^*) = e^{-(E^* - B_n - 2T)^2 / 2\sigma^2}, \quad (19)$$

where B_n and T are the neutron separation energy and the temperature of the compound nucleus, respectively, and $\sigma = 2.5$ is considered in our calculation. The survival probability is calculated using the ratio of the partial widths of neutron emission and fission [25],

$$\Gamma_n / \Gamma_f = \frac{4A^{2/3}(E^* - B_n)}{k(2[a(E^* - B_f)]^{1/2} - 1)} \exp[2a^{1/2}((E^* - B_n)^{1/2} - (E^* - B_f)^{1/2})]. \quad (20)$$

TABLE III. Level density parameter a , P_{CN} , quasifission barrier B_{qf} , and survival probability W_{sur}^1 are our calculated results and W_{sur}^2 are taken from Ref. [25].

Reactions	a (MeV $^{-1}$)	E^* (MeV)	B_{qf} (MeV)	P_{CN}	W_{sur}^1	W_{sur}^2
$^{70}\text{Zn} + ^{208}\text{Pb} \rightarrow ^{277}\text{Cn} + 1n$	26.98	9.8	1	1.52×10^{-7}	7.5×10^{-4}	6×10^{-4}
$^{70}\text{Zn} + ^{209}\text{Bi} \rightarrow ^{278}\text{Nh} + 1n$	27.01	10.6	0.94	3.31×10^{-8}	2.5×10^{-4}	2×10^{-4}
$^{72}\text{Ge} + ^{208}\text{Pb} \rightarrow ^{279}\text{Fl} + 1n$	27.04	12.6	0.77	2.67×10^{-8}	3×10^{-3}	–
$^{74}\text{Ge} + ^{208}\text{Pb} \rightarrow ^{281}\text{Fl} + 1n$	27.14	12.5	0.83	1.47×10^{-8}	3×10^{-3}	2×10^{-3}
$^{76}\text{Ge} + ^{208}\text{Pb} \rightarrow ^{283}\text{Fl} + 1n$	27.24	12.4	0.89	3.79×10^{-9}	2.22×10^{-2}	2×10^{-2}
$^{84}\text{Kr} + ^{208}\text{Pb} \rightarrow ^{291}\text{Og} + 1n$	28.47	12.5	0.45	9.67×10^{-11}	1.18×10^{-2}	2×10^{-2}
$^{86}\text{Kr} + ^{208}\text{Pb} \rightarrow ^{293}\text{Og} + 1n$	28.57	13.3	0.52	1.2×10^{-10}	2.34×10^{-2}	2×10^{-2}
$^{88}\text{Kr} + ^{208}\text{Pb} \rightarrow ^{295}\text{Og} + 1n$	28.67	12	0.58	2.88×10^{-11}	7×10^{-2}	8×10^{-2}
$^{90}\text{Kr} + ^{208}\text{Pb} \rightarrow ^{297}\text{Og} + 1n$	29.12	13.1	0.65	8.6×10^{-12}	4×10^{-2}	5×10^{-2}
$^{92}\text{Kr} + ^{208}\text{Pb} \rightarrow ^{299}\text{Og} + 1n$	29.95	12.4	0.71	4.64×10^{-12}	3.5×10^{-2}	4×10^{-2}

In this equation B_n is the neutron binding energy and $k = 9.8$ MeV. B_f is evaluated using $B_f = B_f(E = 0) \exp[-E/E_d]$, where $B_f(E = 0)$ is the microscopic correction and the shell damping energy, E_d is defined by $E_d = 0.4A^{4/3}/a$. The nuclear temperature T is

$$T = \left(\frac{\partial S}{\partial E} \right)^{-1}, \quad (21)$$

where S is the entropy and is defined as follows:

$$S(E) = k_B \ln \frac{\rho(E)}{\rho_0}. \quad (22)$$

Here, ρ_0 is the normalization constant and can be evaluated using the third law of thermodynamics. The temperature dependent pairing energy back-shifted Fermi gas (TDP-BSFG) model [29] is used to calculate nuclear level density, $\rho(E)$. In this approach, the nuclear temperature is defined by

$$\frac{1}{T} = \left(\sqrt{\frac{a}{U}} - \frac{3}{2U} \right) \left(1 - \frac{d\Delta(T)}{dT} \frac{dT}{dE} \right), \quad (23)$$

where a is the level density parameter and is calculated using the single particle level density [54]. $\Delta(T)$ is defined based on the EGL theory [55],

$$\Delta(T) = \frac{T_c \pi^2 \int_0^\infty \lambda^{\frac{1}{2}} e^{-\left(\pi \sqrt{\frac{\lambda}{18}} + \frac{\pi(\lambda-1)}{2\sqrt{18\lambda}} \right)^2} d\lambda}{\sqrt{\frac{\delta\pi}{2b}} t^{\frac{1}{2}} \left(1 \pm \text{erf} \left(\left| \frac{\Delta}{t^{\frac{1}{2}}} \right| \right) \right)}, \quad (24)$$

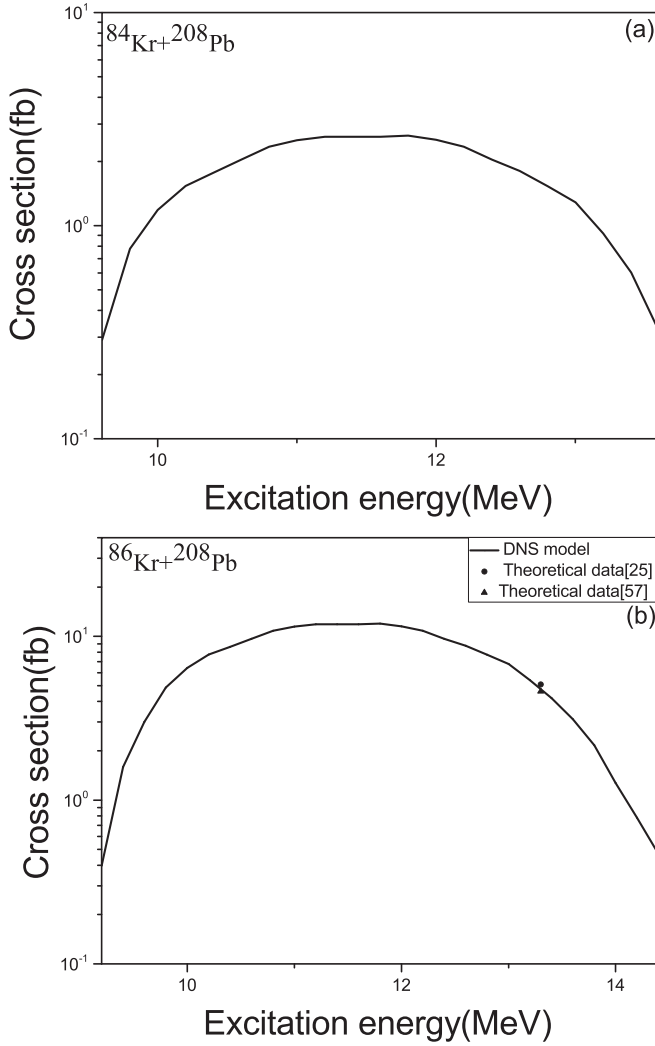


FIG. 5. Evaporation residue cross section as a function of excitation energy for (a) $^{84}\text{Kr} + ^{208}\text{Pb}$ and (b) $^{86}\text{Kr} + ^{208}\text{Pb}$ reactions.

where in the denominator, the plus sign is used for $T < T_c$ and minus sign is for $T > T_c$. The single particle spacing of energy levels (δ) is defined as

$$\delta = \frac{1}{2} \left(\frac{1}{g_p(\epsilon_p^F)} + \frac{1}{g_n(\epsilon_n^F)} \right). \quad (25)$$

In this equation $\bar{\Delta}t = \frac{1}{2}\pi(t-1)/(\bar{b}\bar{\delta})^{\frac{1}{2}}$, $t = \frac{T}{T_c}$, $\bar{b} = 0.526$, $\bar{\delta} = \delta/k_B T_c$, and $\Delta(T)$ is normalized to the value of pairing energy at zero temperature that is calculated based on the liquid drop model. To solve Eq. (23), the excitation energy, $E(T)$, is considered as a complete set of power series up to the third power of nuclear temperature,

$$E(T) = a_0 + a_1 T^1 + a_2 T^2 + a_3 T^3, \quad (26)$$

four constant coefficients, $a_0 \dots a_3$ are obtained by the substitution of $E(T)$ from Eq. (26) into Eq. (23) in each small interval of temperature. Then the temperature is obtained by the iteration method.

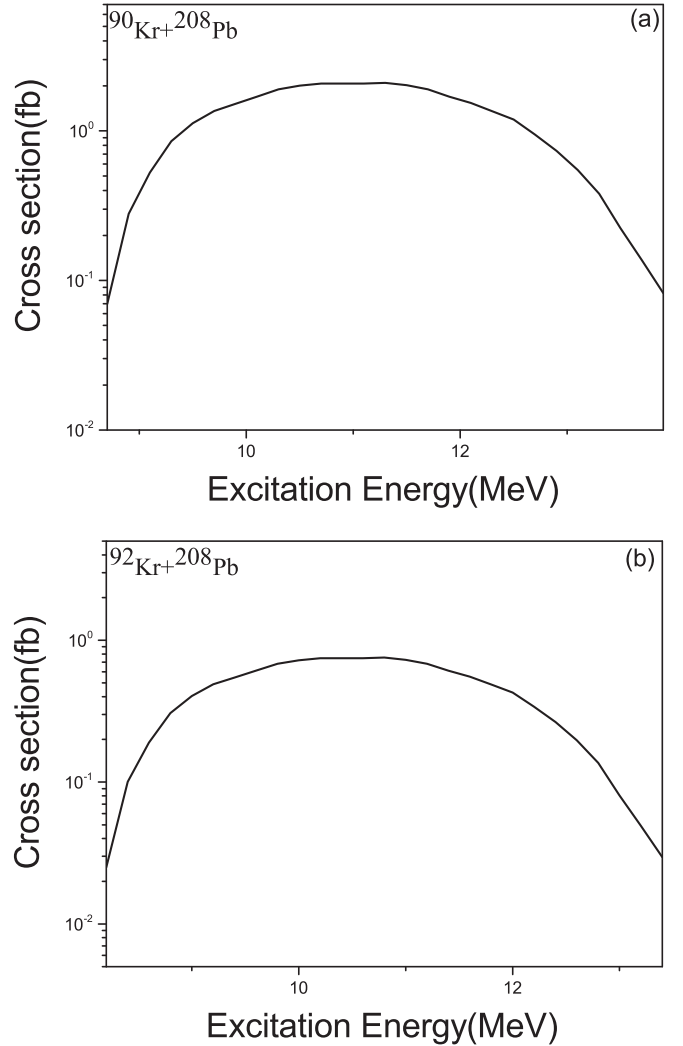


FIG. 6. Evaporation residue cross section as a function of excitation energy for (a) $^{90}\text{Kr} + ^{208}\text{Pb}$ and (b) $^{92}\text{Kr} + ^{208}\text{Pb}$ reactions.

III. RESULTS AND DISCUSSION

In order to evaluate the evaporation residue cross section, the temperature of the compound nucleus is required. Therefore, the temperatures are evaluated using Eq. (21) based on the TDP-BSFG model. The calculated temperature of the compound nucleus as a function of excitation energy is indicated in Fig. 1(a) and 1(b). In order to obtain B_{fus}^* and B_{qf} , the nucleus-nucleus potential and potential energy of DNS, $[U(R) = U(R = R_m, \eta, J)]$ are plotted as a function of R and η for each isotope. One such graph is presented in Figs 2 and 3 in which each η corresponds to a reaction. For each reaction, $R = R_m$ has been obtained by plotting the nucleus-nucleus potential using Eq. (13), as indicated in Fig. 2. The quadrupole, octupole, hexadecapole, and hexacontatetrapole deformations are considered in the calculation (if any) and corresponding deformation parameters (β_2 , β_3 , β_4 , and β_6) for interacting isotopes [56] are listed in Table I.

Despite the lack of experimental data for Og isotopes, the calculated formation cross section of $^{70}\text{Zn} + ^{208}\text{Pb} \rightarrow ^{278}\text{Cn}$ and $^{70}\text{Zn} + ^{209}\text{Bi} \rightarrow ^{279}\text{Nh}$ reactions are compared with

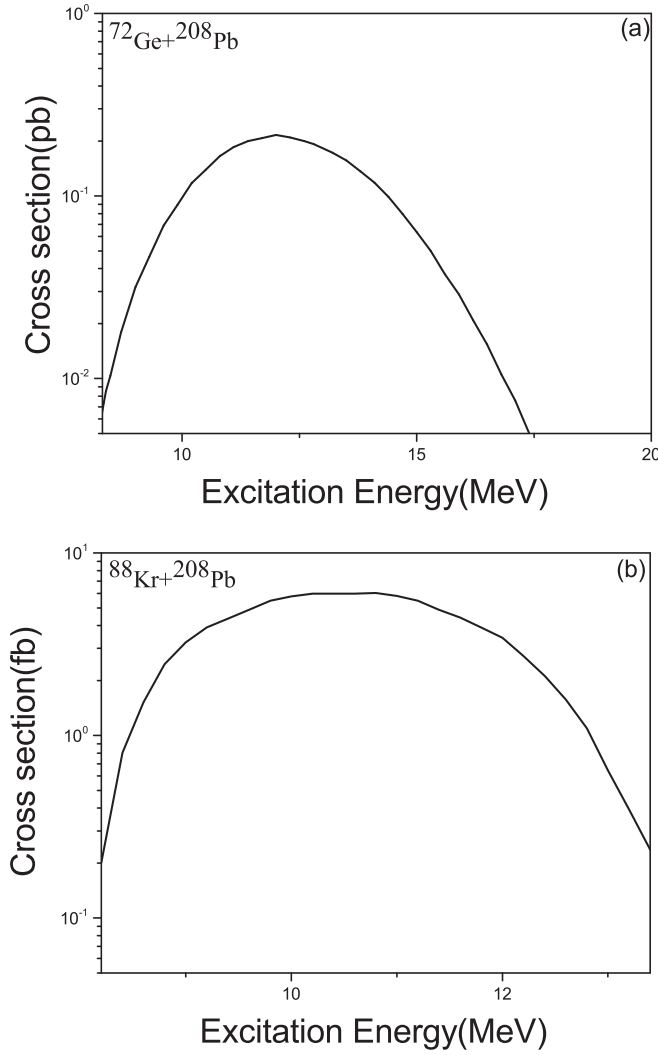


FIG. 7. Evaporation residue cross section as a function of excitation energy for (a) $^{72}\text{Ge} + ^{208}\text{Pb}$ and (b) $^{88}\text{Kr} + ^{208}\text{Pb}$ reactions.

experimental data in Fig. 4. Finally, the formation cross section of Og and Fl SHN isotopes that are produced through following reactions: $^{84}\text{Kr} + ^{208}\text{Pb} \rightarrow ^{292}\text{Og}$, $^{86}\text{Kr} + ^{208}\text{Pb} \rightarrow ^{294}\text{Og}$, $^{88}\text{Kr} + ^{208}\text{Pb} \rightarrow ^{296}\text{Og}$, $^{90}\text{Kr} + ^{208}\text{Pb} \rightarrow ^{298}\text{Og}$, $^{92}\text{Kr} + ^{208}\text{Pb} \rightarrow ^{300}\text{Og}$, $^{72}\text{Ge} + ^{208}\text{Pb} \rightarrow ^{280}\text{Fl}$, $^{74}\text{Ge} + ^{208}\text{Pb} \rightarrow ^{282}\text{Fl}$, $^{76}\text{Ge} + ^{208}\text{Pb} \rightarrow ^{284}\text{Fl}$ are calculated using Eq. (2) and the results are indicated in Figs. 5–8. As mentioned earlier, quantities B_{fus}^* and B_{qf} are calculated from the plots of potential energy and nucleus-nucleus potential (Figs. 2 and 3), respectively. It should be noted that these calculated quantities and the choice of parameters considered in our calculations, for instance, level density parameter, a and Γ may affect the survival probability, P_{CN} and consequently the formation cross section. Numerical results of these quantities are also listed in Table II. The excitation energy, the calculated formation cross section based on the approach used in this research, and theoretical results of other models [25] have been listed in the second, third, fourth, and fifth columns of Table II, respectively. One can see that the calculated results using TDP-BSFG are in good agreement with the theoretical results of other models as well as with the experimental data.

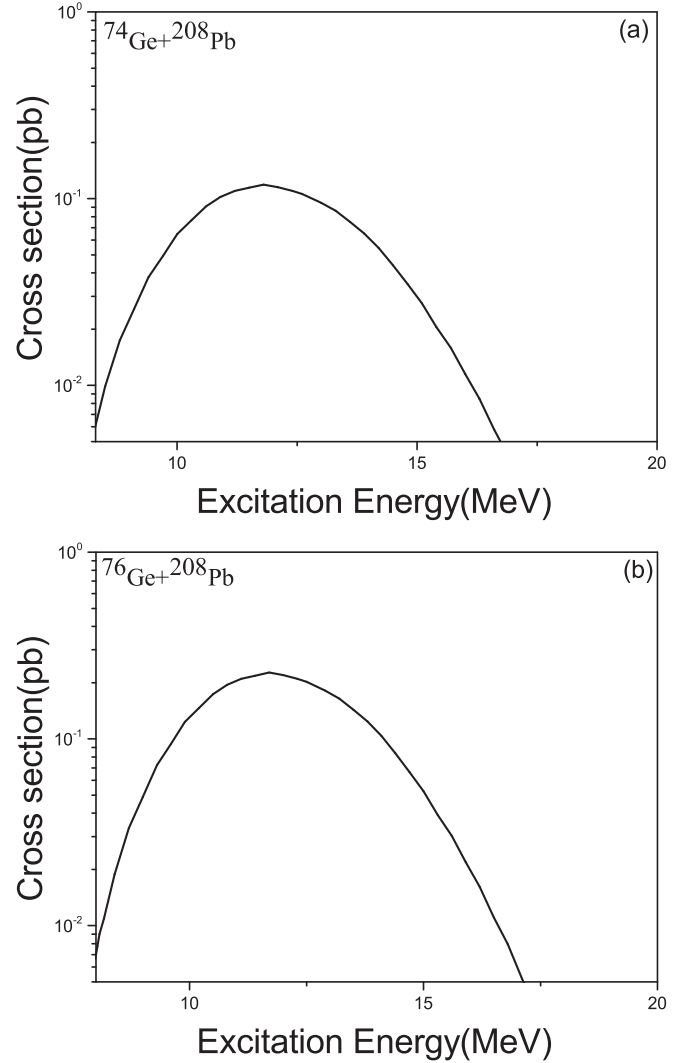


FIG. 8. Evaporation residue cross section as a function of excitation energy for (a) $^{74}\text{Ge} + ^{208}\text{Pb}$ and (b) $^{76}\text{Ge} + ^{208}\text{Pb}$ reactions.

Also for the reaction $^{86}\text{Kr} + ^{208}\text{Pb} \rightarrow ^{294}\text{Og}$, the calculated formation cross section from Refs. [57] and [25] are added for comparison. As it is clear, our calculated formation cross section is highly close to other theoretical results for this reaction. The fusion probability, P_{CN} for these reactions is indicated in Table III.

It can be observed that for these reactions P_{CN} decreases by increasing the level density parameter except for the reaction $^{86}\text{Kr} + ^{208}\text{Pb} \rightarrow ^{294}\text{Og}$, that P_{CN} increases by increasing the level density parameter. Because the level density parameter is related to nuclear temperature therefore it affects the fusion probability through the Kramers rate. But in the case of reaction that produced ^{294}Og isotope, the neutron number of the projectile is equal to a magic number, the variation of fusion probability is reversed. Since the value of $V(R_m)$ decreases due to the deformation effect near $\eta = \eta_{BG}$, causing a decrease to the value of B_{fus}^* , and this increases the P_{CN} [21], but for other reactions deformation effects cause an increase in B_{fus}^* and as a result, a decreasing of P_{CN} . The shell effects are affected through the calculation of fusion barrier

distribution, because for magic closed shell nuclei, the binding energy increases sufficiently which causes an increase in the reaction Q value. Synonymously, increasing the B_{fus}^* causes the frequencies of DNS ($\omega_i^{B_j}$ and ω_i) to vary which can affect the fusion probability. Since the potential energy of the DNS depends on the shell effects, the shell correction affects oscillator frequencies through potential energy. Thus, the variation in fusion probability can be explained by the two factors in Eq. (4), namely, B_{fus}^* and oscillator frequencies which in the case of the $^{86}\text{Kr} + ^{208}\text{Pb} \rightarrow ^{294}\text{Og}$ reaction, the shell effect was found to increase the fusion probability. This behavior is in agreement with the result of Ref. [25] and the result for $^{82}\text{Se} + ^{138}\text{Ba}$ and $^{82}\text{Se} + ^{134}\text{Ba}$ reactions [58], because there is no fusion hindrance for the $^{82}\text{Se} + ^{138}\text{Ba}$ reaction because of the shell closure $N = 82$, thus the shell closure enhances fusion probability. The calculated survival probabilities are compared with the results of Ref. [25]. One can see that our calculated data are close to other theoretical data.

IV. CONCLUSION

In this paper, the evaporation residue cross section is calculated for the following cold reactions: $^{84}\text{Kr} + ^{208}\text{Pb} \rightarrow$

^{292}Og , $^{86}\text{Kr} + ^{208}\text{Pb} \rightarrow ^{294}\text{Og}$, $^{88}\text{Kr} + ^{208}\text{Pb} \rightarrow ^{296}\text{Og}$, $^{90}\text{Kr} + ^{208}\text{Pb} \rightarrow ^{298}\text{Og}$, $^{92}\text{Kr} + ^{208}\text{Pb} \rightarrow ^{300}\text{Og}$, $^{72}\text{Ge} + ^{208}\text{Pb} \rightarrow ^{280}\text{Fl}$, $^{74}\text{Ge} + ^{208}\text{Pb} \rightarrow ^{282}\text{Fl}$, and $^{76}\text{Ge} + ^{208}\text{Pb} \rightarrow ^{284}\text{Fl}$ using the TDP-BSFG model based on the DNS approach. The TDP-BSFG model is used to calculate the level density and the nuclear temperature for ^{292}Og , ^{294}Og , ^{296}Og , ^{298}Og , ^{300}Og , ^{280}Fl , ^{282}Fl , and ^{284}Fl isotopes. In order to calculate fusion probability, the level density parameter is evaluated using the semiclassical method. Then the fusion probability, P_{CN} , and survival cross section are evaluated. It was shown that the calculated survival probability in our approach and the other theoretical model are approximately similar. Also, the fusion probability for the reaction $^{86}\text{Kr} + ^{208}\text{Pb} \rightarrow ^{294}\text{Og}$ is maximum, while for other reactions, P_{CN} decreases by reducing η . This effect can be described by the deformation of the nuclei in the initial DNS and DNS at the top of the barrier in η and by the shell effects. Moreover, to examine our approach the calculated evaporation residue cross section of $^{70}\text{Zn} + ^{208}\text{Pb} \rightarrow ^{278}\text{Cn}$ and $^{70}\text{Zn} + ^{209}\text{Bi} \rightarrow ^{279}\text{Nh}$ reactions are calculated and compared with experimental data. One can see that our results are in good agreement with the experimental data.

-
- [1] E. Fermi, Possible production of elements of atomic number higher than 92, *Nature* **133**, 898 (1934).
- [2] S. Hofmann and G. Munzenberg, The discovery of the heaviest elements, *Rev. Mod. Phys.* **72**, 733 (2000).
- [3] A. K. Nasirov, G. Giardina, G. Mandaglio, M. Manganaro, F. Hanappe, S. Heinz, S. Hofmann, A. I. Muminov, and W. Scheid, Quasi-fission and fusion-fission in reactions with massive nuclei: Comparison of reactions leading to the $Z=120$ element, *Phys. Rev. C* **79**, 024606 (2009).
- [4] Y. Arimoto, Fusion hindrance and roles of shell effects in superheavy mass region, *Nucl. Phys. A* **780**, 222 (2006).
- [5] B. B. Back, H. Esbensen, C. L. Jiang, and K. E. Rehm, Recent developments in heavy-ion fusion reactions, *Rev. Mod. Phys.* **86**, 317 (2014).
- [6] S. Hofmann, New elements - approaching, *Rep. Prog. Phys.* **61**, 639 (1998).
- [7] Z. Patyk and A. Sobiczewski, Ground-state properties of the heaviest nuclei analyzed in a multidimensional deformation space, *Nucl. Phys. A* **533**, 132 (1991).
- [8] W. J. Swiatecki, Systematics of spontaneous fission half-lives, *Phys. Rev.* **100**, 937 (1955).
- [9] G. N. Flerov and G. M. Ter-Akopian, Synthesis and study of atomic nuclei with $Z > 100$, *Prog. Part. Nucl. Phys.* **19**, 197 (1988).
- [10] Yu. Ts. Oganessian *et al.*, Synthesis of Superheavy Nuclei in the $^{48}\text{Ca} + ^{244}\text{Pu}$ Reaction, *Phys. Rev. Lett.* **83**, 3154 (1999); Synthesis of nuclei of the superheavy element 114 in reactions induced by ^{48}Ca , *Nature* **400**, 242 (1999); Y. T. Oganessian, V. K. Utyonkov, and K. J. Moody, Synthesis of $^{252}116$ in the $^{248}\text{Cm} + ^{48}\text{Ca}$ reactions, *Phys. Atom. Nucl.* **64**, 1349 (2001) [From *Yadernaya Fizika* 63, 1769 (2000)].
- [11] Yu. Ts. Oganessian, V. K. Utyonkov, Y. V. Lobanov *et al.*, Observation of the decay of $^{292}116$, *Phys. Rev. C* **63**, 011301(R) (2000).
- [12] S. Hofmann, D. Ackermann, A. V. Yeremin *et al.*, The reaction $^{48}\text{Ca} + ^{238}\text{U} \rightarrow ^{286}112^*$ studied at the GSI-SHIP, *Eur. Phys. J. A* **32**, 251 (2007).
- [13] Yu. Ts. Oganessian, V. K. Utyonkov, Yu. V. Lobanov, F. Sh. Abdullin, A. N. Polyakov, R. N. Sagaidak, I. V. Shirokovsky, Yu. S. Tsyganov *et al.*, Synthesis of the isotopes of elements 118 and 116 in the ^{249}Cf and $^{245}\text{Cm} + ^{48}\text{Ca}$ fusion reactions, *Phys. Rev. C* **74**, 044602 (2006).
- [14] R. Smolańczuk, Formation of superheavy elements in cold fusion reactions, *Phys. Rev. C* **63**, 044607 (2001).
- [15] P. Frobrich and I. I. Gontchar, Langevin description of fusion, deep-inelastic collisions and heavy-ion-induced fission, *Phys. Rep.* **292**, 131 (1998).
- [16] S. M. Mirfathi and M. R. Pahlavani, Dynamical simulation of energy dissipation in asymmetric heavy-ion induced fission of ^{200}Pb , ^{213}Fr , and ^{251}Es , *Phys. Rev. C* **78**, 064612 (2008).
- [17] V. V. Volkov, Process of complete fusion of nuclei. Nuclear fusion within the dinuclear-system concept, *Phys. Part. Nucl.* **35**, 425 (2004).
- [18] H. C. Manjunatha and K. N. Sridhar, Projectile target combination to synthesis superheavy nuclei $Z = 126$, *Nucl. Phys. A* **962**, 7 (2017).
- [19] N. V. Antonenko, E. A. Cherepanov, A. K. Nasirov, V. B. Permjakov, and V. V. Volkov, Competition between complete fusion and quasi-fission in reactions between massive nuclei. The fusion barrier, *Phys. Lett. B* **319**, 425 (1993); Compound nucleus formation in reactions between massive nuclei: Fusion barrier, *Phys. Rev. C* **51**, 2635 (1995).
- [20] G. G. Adamian, N. V. Antonenko, and W. Scheid, Model of competition between fusion and quasifission in reactions with heavy nuclei, *Nucl. Phys. A* **618**, 176 (1997).
- [21] G. G. Adamian, N. V. Antonenko, W. Scheid, and V. V. Volkov, Treatment of competition between complete fusion and quasi-fission in collisions of heavy nuclei, *Nucl. Phys. A* **627**, 361 (1997).

- [22] N. V. Antonenko, G. G. Adamian, W. Scheid, and V. V. Volkov, Competition between complete fusion and quasifission in reactions with heavy nuclei, *AIP Conf. Proc.* **425**, 51 (1998); G. G. Adamian, Competition between complete fusion and quasi-fission in di-nuclear system, *Nuovo Cimento A* **110**, 1143 (1997).
- [23] R. V. Jolos, A. K. Nasirov, and A. I. Muminov, The role of the entrance channel in the fusion of massive nuclei, *Eur. Phys. J. A* **4**, 245 (1999).
- [24] Z.-Q. Feng, G.-M. Jin, and J.-Q. Li, Production of new superheavy $Z=108-114$ nuclei with ^{238}U , ^{244}Pu , and $^{248,250}\text{Cm}$ targets, *Phys. Rev. C* **80**, 057601 (2009).
- [25] G. G. Adamian, N. V. Antonenko, and W. Scheid, Isotopic dependence of fusion cross sections in reactions with heavy nuclei, *Nucl. Phys. A* **678**, 24 (2000).
- [26] A. Bohr and B. R. Mottelson, *Nuclear Structure*, Vol. I (Benjamin, Reading MA, 1969).
- [27] T. Von Egidy, H. H. Schmidt, and A. N. Behkami, Nuclear level densities and level spacing distributions: Part II, *Nucl. Phys. A* **481**, 189 (1988).
- [28] T. Von Egidy and D. Bucurescu, Systematics of nuclear level density parameters, *Phys. Rev. C* **72**, 044311 (2005); Erratum: Systematics of nuclear level density parameters [72, 044311 (2005)], **73**, 049901(E) (2006).
- [29] A. J. Koning, S. Hilaire, and S. Goriely, Global and local level density models, *Nucl. Phys. A* **810**, 13 (2008).
- [30] A. Gilbert and A. G. W. Cameron, A composite nuclear-level density formula with shell corrections, *Can. J. Phys.* **43**, 1446 (1965).
- [31] S. E. Koonin, D. J. Dean, and K. Langanke, Shell model Monte Carlo methods, *Phys. Rep.* **278**, 1 (1997).
- [32] Y. Alhassid, G. F. Bertsch, and L. Fang, Nuclear level statistics: Extending shell model theory to higher temperatures, *Phys. Rev. C* **68**, 044322 (2003).
- [33] R. Razavi, A. N. Behkami, and V. Dehghani, Pairing phase transition and thermodynamical quantities in $^{148,149}\text{Sm}$, *Nucl. Phys. A* **930**, 57 (2014).
- [34] G. Puddu, P. F. Bortignon, and R. A. Broglia, The RPA-SPA approximation to level densities, *Ann. Phys. (NY)* **206**, 409 (1991).
- [35] H. Attias and Y. Alhassid, The perturbed static path approximation at finite temperature: Observables and strength functions, *Nucl. Phys. A* **625**, 565 (1997).
- [36] N. J. Davidson, S. S. Hsiao, J. Markram, H. G. Miller, and Y. Tzeng, A semi-empirical determination of the properties of nuclear matter, *Phys. Lett. B* **315**, 12 (1993).
- [37] L. G. Moretto, Statistical description of a paired nucleus with the inclusion of angular momentum, *Nucl. Phys. A* **185**, 145 (1972).
- [38] E. G. Ryabov, A. V. Karpov, P. N. Nadtochy, and G. D. Adeev, Application of a temperature-dependent liquid-drop model to dynamical Langevin calculations of fission-fragment distributions of excited nuclei, *Phys. Rev. C* **78**, 044614 (2008).
- [39] L. D. Landau and E. M. Lifshitz, *Statistical Physics* (Pergamon Press, Oxford, 1966).
- [40] P. Mohammadi, V. Dehghani, and A. A. Mehammandoost-Khajeh-Dad, Applying modified Ginzburg-Landau theory to nuclei, *Phys. Rev. C* **90**, 054304 (2014).
- [41] M. K. G. Kruse, H. G. Miller, A. R. Plastino, A. Plastino, and S. Fujita, Landau-Ginzburg method applied to finite fermion systems: Pairing in nuclei, *Eur. Phys. J. A* **25**, 339 (2005).
- [42] A. S. Zubov, G. G. Adamian, and N. V. Antonenko, Application of statistical methods for analysis of heavy-ion reactions in the framework of a dinuclear system model, *Phys. Part. Nucl.* **40**, 847 (2009).
- [43] G. G. Adamian, N. V. Antonenko, W. Scheid, and V. V. Volkov, Fusion cross sections for superheavy nuclei in the dinuclear system concept, *Nucl. Phys. A* **633**, 409 (1998).
- [44] G. Munzenberg, Recent advances in the discovery of transuranium elements, *Rep. Prog. Phys.* **51**, 57 (1988).
- [45] G. G. Adamian, N. V. Antonenko, A. Diaz Torres, W. Scheid, and Yu M. Tchuvil, Fusion and quasifission in collisions of heavy nuclei, *AIP Conf. Proc.* **561**, 421 (2001).
- [46] C. Y. Wong, Interaction Barrier in Charged-Particle Nuclear Reactions, *Phys. Rev. Lett.* **31**, 766 (1973).
- [47] L. C. Chamon, G. P. A. Nobre, D. Pereira, E. S. Rossi, Jr., C. P. Silva, L. R. Gasques, and B. V. Carlson, Coulomb and nuclear potentials between deformed nuclei, *Phys. Rev. C* **70**, 014604 (2004).
- [48] Sh Hamada, I. Bondok, and M. Abdelmoatmed, Double folding potential of different interaction models for $^{16}\text{O} + ^{12}\text{C}$. Elastic Scattering, *Braz. J. Phys.* **46**, 740 (2016).
- [49] Z. Gao-Long, Z. Huan Qiao, L. Zu-Hua, Z. Chun-Lei *et al.*, Calculation of interaction potentials between spherical and deformed nuclei, *Chin. Phys. Lett.* **24**, 397 (2007).
- [50] G. G. Adamian, N. V. Antonenko, R. V. Jolos *et al.*, Effective nucleus-nucleus potential for calculation of potential energy of a dinuclear system, *Int. J. Mod. Phys. E* **5**, 191 (1996).
- [51] B. Buck, H. Friedrich, and C. Wheatley, Local potential models for the scattering of complex nuclei, *Nucl. Phys. A* **275**, 246 (1977).
- [52] I. I. Gontchar, D. J. Hinde, M. Dasgupta, and J. O. Newton, Double folding nucleus-nucleus potential applied to heavy-ion fusion reactions, *Phys. Rev. C* **69**, 024610 (2004).
- [53] Z.-Q. Feng, G.-M. Jin, J.-Q. Li, and W. Scheid, Formation of superheavy nuclei in cold fusion reactions, *Phys. Rev. C* **76**, 044606 (2007).
- [54] M. R. Pahlavani and M. Masoumi Dinan, Thermal properties of ^{172}Yb and ^{162}Dy isotopes in the back-shifted Fermi gas model with temperature-dependent pairing energy, *Pramana J. Phys.* **93**, 37 (2019).
- [55] S. A. Alavi and V. Dehghani, Nuclear level density of even-even nuclei with temperature-dependent pairing energy, *Eur. Phys. J. A* **53**, 306 (2016).
- [56] P. Moller, J. R. Nix, W. D. Myers, and W. J. Swiatecki, Nuclear ground state masses and deformations, *At. Data Nucl. Data Tables* **59**, 185 (1995).
- [57] G. Giardina, S. Hofmann, A. I. Muminov, and A. K. Nasirov, Effect of the entrance channel on the synthesis of superheavy elements, *Eur. Phys. J. A* **8**, 205 (2000).
- [58] Bao-An Bian, Feng-Shou Zhang, and Hong-Yu Zhou, Effect of shell structure in the fusion reactions, *Eur. Phys. J. A* **43**, 67 (2010).
- [59] S. Hofmann, F. P. Heßberger, D. Ackermann, G. Münzenberg *et al.*, New results on elements 111 and 112, *Eur. Phys. J. A* **14**, 147 (2002).
- [60] K. Morita, K. Morimoto, D. Kaji, T. Akiyama *et al.*, Experiment on the synthesis of element 113 in the reaction $^{209}\text{Bi}(^{70}\text{Zn}, n)^{278}113$, *J. Phys. Soc. Jpn.* **73**, 2593 (2004).